BN5101 Final Report

COllapsible Mount for TRAnscranial Doppler (COMTRAD)

Team FIT

Flynn Loh Jian Long (A0166755R)

Irvin Lim (A0173028J)

Tianyu Sun (A0167233H)

Table of Contents

1 Abstract

Background: The transcranial doppler (TCD) ultrasound is the current gold standard for determining cerebral blood flow velocity (CBFV) in patients, which serves as a crucial parameter in early ischemic stroke detection. However, the absence of trained operators in ambulatory settings meant that early detection is difficult.

Method: The proposed device, **COllapsible Mount for TRAnscranial Doppler (COMTRAD)**, is a TCD probe holder and mount that can be attached to the temporal window on the patient's head and perform automatic searching for the patient's mid cerebral artery (MCA) to register the CBFV signal required for early detection. The COMTRAD also stabilises the TCD probe in position once the signal is found for prolonged monitoring in the ambulance. A low-fidelity prototype is constructed to test for the validity of fundamental probe holder movements and the viability of the probe holder movements involved in the auto-searching process.

Results: The scanning area covered by the probe is 7 cm^2. The probe holder movement speed is approximately 3.14 cm/s. The translation and rotation mechanisms of the probe holder (4 DOFs) are valid. The translational and rotational phases of the scanning protocol are viable. Refer to supplementary video for the test on probe holder movements.

Discussion: Future characterization (of the rotary motors and probe holder movement) and system evaluation is needed before the COMTRAD can be deployed. Potential development in the rigidization, the actuation, and the functionality of the COMTRAD were put forth.

2 Background

In Singapore alone, the prevalence of stroke has had a significant increase from 187.9 to 229.6 per 100,000 over a ten year period from 2008 to 2017 [1]. While heart attacks have been able to be diagnosed in a pre-hospital setting to the extent that a non-medical-professional is able to follow specific instructions to use an AED that can diagnose and administer defibrillating shocks, there is no equivalent for the diagnosis of strokes. An Australian study by Bray et al. reported that out of 5286 emergency transports, approximately 16% of the patients were tested for strokes [2], which holds a significant proportion of emergency patients. The current gold standard for the diagnosis of strokes is the use of a Transcranial Doppler (TCD) ultrasound machine to detect the presence of a blood flow in the mid cerebral artery (MCA). As approximately 80% of strokes are ischemic (due to thrombosis or embolism) [3], the change in the cerebral blood flow velocity (CBFV), obtained via the TCD reading, can be indicative of the ischemic stroke and thus aid in stroke diagnosis.

The TCD exam approaches and relevant cerebral artery information (and abbreviations) can be found in the supplementary information under *Natus TCD Summary*. As will be expounded later, the TCD presents its set of bottlenecks with the need for a trained radiologist to operate the device. As this is not currently possible, the TCD is not able to be deployed in a pre-hospital environment.

2.1 Locating and Imaging The MCA

The probe has to be positioned optimally to image the MCA and this is accomplished by a trained radiologist in two steps. First, locating the temporal window, which is a position on the temple that is conducive for the imaging of the MCA by virtue of the individual's unique skull structure. When translating into mechanical requirements this will entail translational movement of the probe across the surface of the patient's head. After locating the temporal window, the probe will then have to be angled such that it is acquiring the maximum signal from the doppler ultrasound [4]. This angle in question is termed the insonation angle and determines the strength and accuracy of the signal. In mechanical terms this would mean rotations in the planes orthogonal to the surface of the head.

2.2 Stabilisation from External Perturbations

It may seem superfluous to be designing yet another device to combat a problem for which there are existing solutions, as will be touched upon in the Section 4.1 on existing solutions, but in this section the current problem shall be defined through explanations of why current devices are as yet insufficient to meet requirements of our purpose which is defined as ambulatory monitoring of the MCA without the need of a skilled operator.

Apart from the clinical requirements in performing a TCD, there exist additional requirements when such a procedure is performed in a pre-hospital setting such as an ambulance [5]. Not only are the placement of the probe on the temporal window and insonation angle required, they are sensitive and are susceptible to external perturbations such as patient movement and movement from the ambulance ride. As such our device needs not only to be able to locate the MCA but also actively correct for external forces that will displace the probe from the temporal window and optimal insonation angle.

3 Aims & Significance

3.1 Aims

We propose a TCD probe holding device: **COllapsible Mount for TRAnscranial Doppler (COMTRAD)**. In subsequent text references, the COMTRAD and the proposed device are referring to the same device. Based on the described problems above, besides being able to act as a TCD probe holder, the COMTRAD should aim to have the corresponding features to achieve the respective objectives. By achieving these aims, the COMTRAD, when deployed, should allow the untrained operator to read the CBFV off the TCD interface. In this section, we elaborate on these target features:

3.1.1 Aim 1: Collapsibility and Mount-ability

The proposed device should be able to collapse and be packed in a convenient manner. The device can then be rigidized in its expanded form when necessary. The architectural design will involve an origami design to fulfil this criterion, with springs in place for the rigidization sequence desired. The proposed device should also be able to mount on the patient's temporal window on the head to secure the device at the location. This is achieved using an adhesive surface at the bottom of the surrounding shell, with the shell attached to a strap configuration for securing the device to the head.

3.1.2 Aim 2: Probe Movement

The proposed device should be able to move the TCD probe in a manner that enables the system to search for the MCA and adjust the angulation for optimal signal, alongside the ability to perform physical stabilization in a vibrational environment and at any mount angle. The design achieves this by using strings and rotary motors for the simplicity, low cost, and effectiveness.

3.1.3 Aim 3: Positional Input

The proposed device should be aware of the spatial position of the TCD probe in relation to the fixed location of the entire device. The sensing method will be achieved using an inertial measurement unit (IMU) attached to the probe holder in the design.

3.1.4 Aim 4: Control System

The proposed device should be able to determine the appropriate translation and angulation movements to achieve probe stability and search for the MCA in the event the signal on the MCA is lost. This is done using a control system that can be situated away from the patient to reduce mass on the set-up mounted on the head.

3.2 Significance

The aims are based on the shortcomings of existing devices and being able to achieve these aims will solve these shortcomings. The solution to these aims can likely be integrated into existing devices that face the shortcomings. Following each aim, the specific significances are as follows:

3.2.1 Significance 1: Collapsibility and Mount-ability

This aim strikes at the heart of our use case: pre-hospital settings. Compared to current devices which are large and cumbersome, a portable device would be novel. Such portability allows it to be used in any pre-hospital setting without needing special preparation much like an AED can simply be stored and used in any setting. The further mount-ability allows the device to be used in mobile settings where the patient has to be moved, likely to a hospital.

3.2.2 Significance 2: Probe Movement

The movement allows the probe to be manipulated to achieve a clear and ideal signal with instruction from the control system. The precision we aim to achieve is a key point of interest for us due to the sensitive nature of the ultrasound signal's relationship to the probe placement. To have accurate and precise probe movement is one key factor that has to be present to replace the operator, the other being the ability to keep the probe holder in place to maintain the signal readout.

3.2.3 Significance 3: Positional Input

Other than recognising an ideal signal, the device needs input via an awareness of the probe relative to the mount. This is analogous to proprioception in a human operator. This will improve the control and effectiveness of the control movement.

3.2.4 Significance 4: Control System

Apart from replacing the physical manipulation by a human operator, the control system is integral in providing effective direction and instruction to the actuators to achieve an ideal signal. The presence of such a control system will replace the recognition of an operator and be the "brain" of our system that is poised to replace a radiologist. Even without the integration of the control system with a physical mount and assembly, the significance still lies in that such a control system can be augmented to instruct an operator of lower skill level than a radiologist, perhaps a paramedic or other first responder, to perform the ischemic stroke detection with TCD.

4 Related Work

This section elaborates on some of the current probe holders proposed in other articles and patents, and potential actuators that could possibly be implemented in the system design. For more details and relevant figures, as well as summary tables for each section, refer to the supplementary information.

4.1 Current Probe Holders

There have been attempts to robotically control the angulation and translation of a TCD probe. The mechanisation of the probe, via a probe holder allows the probe to ultimately be autonomously controlled. Qiu et al. [6] developed a detachable rigid holder for the a TCD probe that is mounted on a bracket that is able to adjust its height and angulation. This gives the probe the ability to translate in 1 dimension and rotate about two axes giving a total of 3 DOFs with respect to the arm which the bracket is mounted on. Molloy et al. [7] developed a wearable TCD device that is worn on the head of the patient. This device is worn such that the probe is placed on the temporal window which has to be pre-identified with a conventional TCD procedure. The device uses an auto-search module to restore vessel insonation, if needed, every 5 minutes. Gomez et al. [4] utilised a housing device that is adhered, with collodion, to the temporal window which has to be pre-identified with a conventional TCD procedure. The housing passively holds the probe stable to ensure continuous ideal signals from the MCA. Sheehan et al. [8] similarly developed a housing that passively holds the TCD probe in place with an external skin ward force via a compression device and strap to minimise air gaps between the probe and the skin. The locking mechanism that holds the device in place is modified to ensure that probe angulation is not affected unintentionally. Just like Molloy's and Gomez's, Sheehan's design requires the temporal window to be pre-identified with a conventional TCD procedure. Njemanze et al. [9] uses a housing that is based on a bitemporal probe hanger to be worn by the patient. The holder that is attached to this hanger is able to perform vessel insonation via electromotive forces and is aware of the probe angle via electromagnetic induction. A neural network is then able to utilise the electromotive force and information from the electromagnetic induction to perform repositioning, insonation, to achieve an ideal signal from the MCA.

4.2 Potential Actuators

In developing a method for the active movement of our probe we had to consider actuators. The two actuators that were shortlisted for use are detailed below.

Suzuki et al. [10] developed a miniature RCM manipulator (mini-RCM), a 5 × 7 × 5 cm 3 DOF mechanism based on parallelogram mechanical linkages. The RCM is actuated by miniature linear actuators (mini-LAs) of 2.8cm × 0.7cm × 0.36cm in size. They exhibit high linearity, can drive a payload of 170 mN and its integrated sensing provides a resolution of 50 microns. Rotational joints are actuated from translation motions by slider crank mechanisms. The mini-LAs function using PZT-based stick-slip mechanism for the large stroke motion and high force-to weight ratio and are controlled in real time by a closed-loop proportional controller. The displacement sensing is done through an optical sensing method for stability against electrical noise. Banjeree et al. [11] utilised a mechanical design with nylon string and springs to generate motion with a single motor. A spring module is assembled with different segments attached together by nylon string this spring module is able to contract as the motor winds the string. Then, the motor would unwind the string and the module would expand to its original state by the extension force provided by the spring. An actuator can consist multiple spring modules and it is programmed by Arduino to repeat the motion such that the actuator is able to generate a peristaltic movement.

Though neither were used in the final product for the use of controlling the movement of the probe holder and thus the probe, the method described by Banjeree et al. [11] was modified to provide the extension and rigidity to the surrounding shell. This is elaborated on in Architecture.

5 Methodology

5.1 System Design

The COMTRAD can be described in four aspects of the proposed device, with each aspect covering an ‘A’ in the ‘AAAA’ design approach[1] of robotic systems. The COMTRAD consists of a set-up (a housing with 8 strings in individual sheaths and an IMU, and head straps) that is mounted onto the temporal window of the patient’s head with adhesive and straps, a flexible cable that holds all the wires and string sheaths connecting to the set-up, and at the other end of the cable, an external unit (containing the microcontroller, 8 rotary motors, and battery) that can be placed away from the patient. The specifications and materials used in the design can be found in the Sections 5.2 and 5.3.

5.1.1 Housing (Architecture)

The housing of the COMTRAD is targeted at achieving Aim 1 (collapsibility and mount-ability). It consists of a surrounding shell and a central probe holder (that is held by 8 strings), as seen in Figure 1. Both surrounding shell and probe holder are able to collapse in their axial direction through a tetragonal bellow fold pattern along the side walls. The fold pattern, based on a pattern used by Schenk et al. for inflatable space structures [12], is illustrated in Figure 2. The origami templates for the side walls of the surrounding shell and the probe holder are provided in the supplementary information. The tetragonal bellow fold pattern was chosen for its minimal fold length and available internal space when the structure is folded, as described by Schenk [12], which would more likely enforce a straight deployment in the axial direction and allow the central probe

[1] ‘AAAA’ represents architecture, actuator, awareness (sensing), and AI.

holder to be stowed together within the shell. When folded, the device has a height of 2 cm, allowing it to be stowed conveniently under the external unit as discussed later.

The side walls of the probe holder and surrounding shell are made of waxed construction paper to retain the crease patterns, provide a strong rigidity and a slight level of water resistance to the structure. When extended, the surrounding shell holds its shape with the help of 4 springs at each corner, as demonstrated in the exploded view of the housing in Figure 3. Each spring, having an original uncompressed length of 15 cm ($>$ 10 cm) and a compression limit of 2 cm, has an internal string of length 10 cm within it to restrict its extension. The 4 springs are situated at the four corners to ensure even extension at every corner. As such, when the housing is compressed, the springs compress to 2 cm (which is also found to be the axial compression limit of the housing); When the housing is extended, the springs can only extend up to 10 cm (restricted by the 10 cm long internal strings) and not its original uncompressed length of 15 cm, thereby providing an outward force on both ends to maintain the structural rigidity of the bellow fold side walls. The approach was adapted from the actuator model developed by Banerjee et al [11]. The side walls of the surrounding shell are attached at the top and bottom to hard plates through which strings pass to control the inner probe holder.

The probe holder is of similar design to the surrounding shell – an extendable bellow fold side wall sandwiched by two hard plates. These hard plates are the points of control, attached to the motors by nylon strings. When in use, the extension of the probe holder is reliant on the extended surrounding shell via the strings and the internal friction between the cavity side walls and the probe. The strings then allow the probe holder (and by extension, the probe) to be moved relative to the surrounding shell, which will be elaborated in Section 5.1.3. The probe holder also features an IMU which can relay information to the off board controller.

When in use, the probe holder will hold a TCD probe and the surrounding shell will be mounted on the temporal window on the patient’s head with a peel-off adhesive and then fastened with a head strap, as seen in Figure 1C. This combines the methods mentioned by Gomez et al. [4] and Sheehan et al. [8] to increase the passive stability that is required in a dynamic pre-hospital setting. Contrasting with the methods described by Gomez et al [4], Molloy et al. [7] and Sheehan et al. [8], the location of the temporal window does not need to be determined (by the operator) with high accuracy as the device is able to produce translation in two axes and angulation about two axes. This allows the device to be placed approximately around the temporal window. The approximate region to attach the housing can be printed onto a pictorial quick guide, much like the diagrams indicating the two locations for the chest pads in an AED. Also, the application of ultrasound gel to the scanning area is necessary before mounting the set-up.

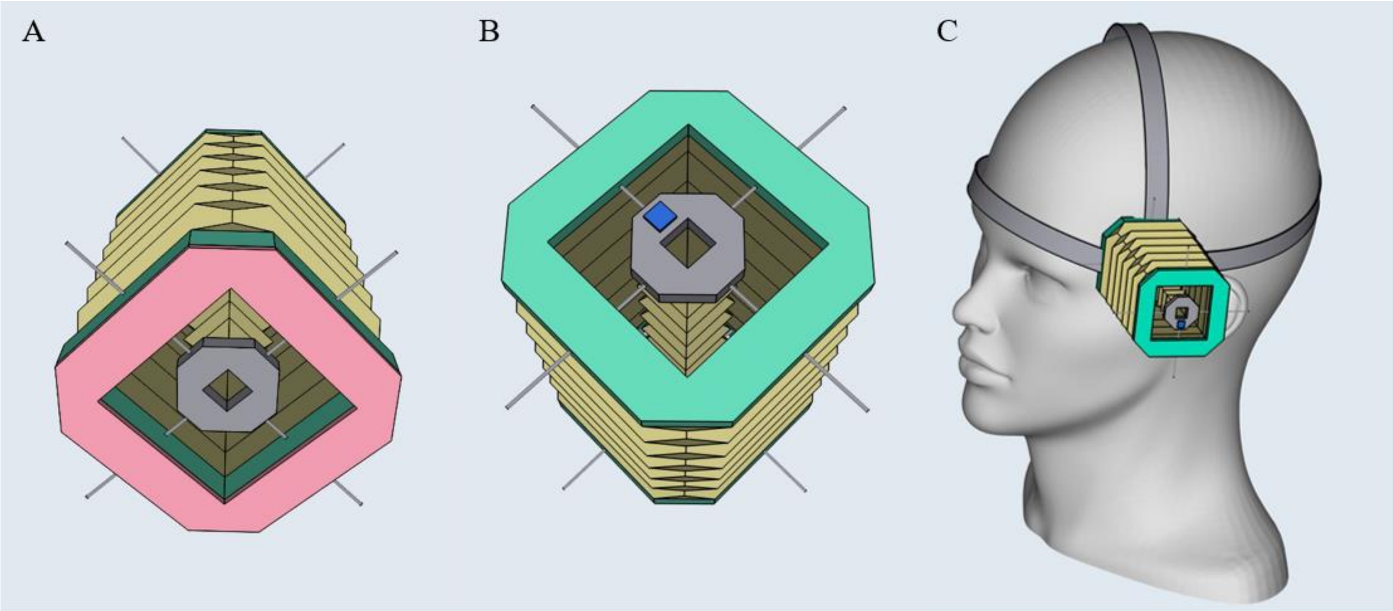

Figure 1. Computer-aided design (CAD) of the housing of the COMTRAD, which consists of a surrounding shell (and its top and bottom hard plates in turquoise), the probe holder (and its top and bottom hard plates in grey), the IMU (installed on the top hard plate of the probe holder, shown in blue), and the 8 strings that are attached to the probe holder and passes through holes in the (top and bottom) hard plates of the surrounding shell. The side walls of the surrounding shell and probe holder (yellow) are constructed with the tetragonal bellow fold (the CAD of the bellow fold is for illustration purposes and not accurate in terms of the fold pattern). The cable that runs from the housing to the external unit is not shown. ***A****: Bottom view of the housing. Pink layer shown is the adhesive layer.* ***B****: Top view of the housing. Blue square shown is the IMU.* ***C****: Set-up mounted onto the temporal window of the patient's head with the bottom adhesive and accompanying head straps.*

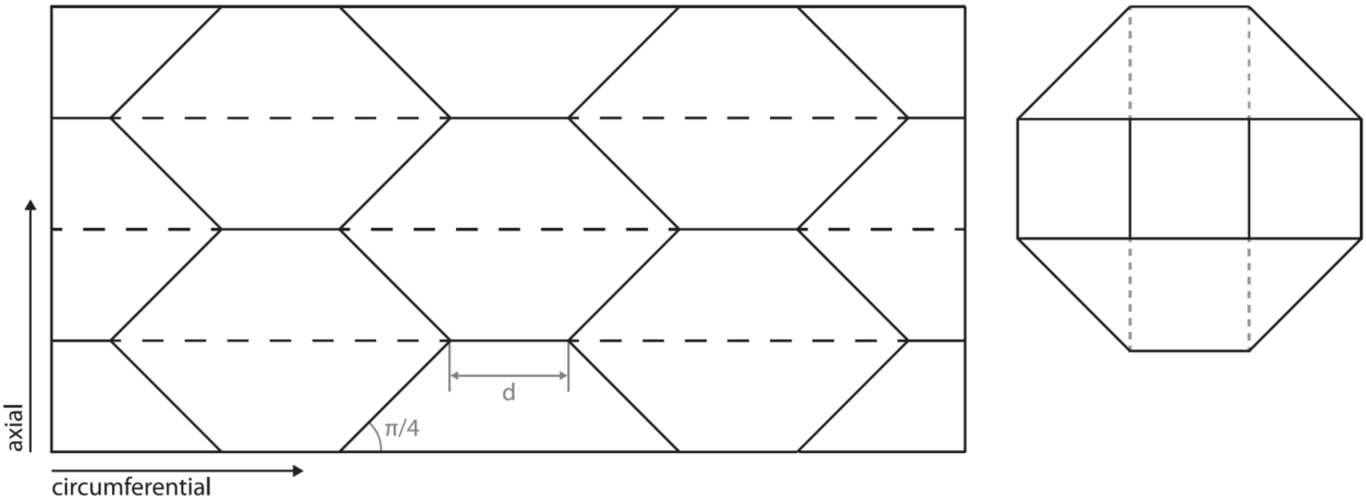

Figure 2: Fold pattern of the tetragonal bellow fold [12] adapted for the housing side walls. The left diagram shows the flat layout of the fold pattern, with dashed lines representing valley folds and the solid lines representing the mountain folds; The right diagram shows the top view of the folded structure. For the templates with the actual dimensions and fold layers, refer to the supplementary information.

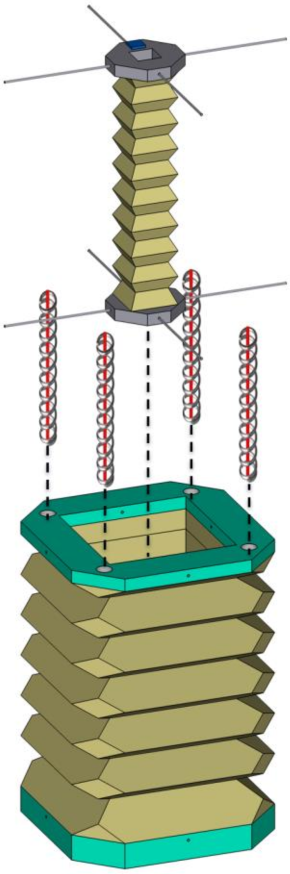

Figure 3: Exploded view of the housing of the COMTRAD. Shown here is the probe holder (and the 8 strings) outside of the surrounding shell. The 4 springs (and its respective internal strings shown in red) that are originally in the side wall of the surrounding shell are exposed as well for illustrative purposes.

5.1.2 External Unit

The external unit in Figure 4 contains the components that need not be mounted on the set-up (housing and head straps) of the COMTRAD. As detailed in Section 5.1.3, the 8 rotary motors are located away from the set-up and will be placed in the external unit along with a 6 volt battery and the Arduino unit. The cables from the motors will be channelled out the side of the external unit to eventually reach the housing of the set-up. The use of an external unit shifts most of the weight away from the set-up to keep it lightweight. Additionally, leveraging the main unit's collapsibility, the external unit has additional storage attachments underneath where the collapsed housing can be stored when not in use.

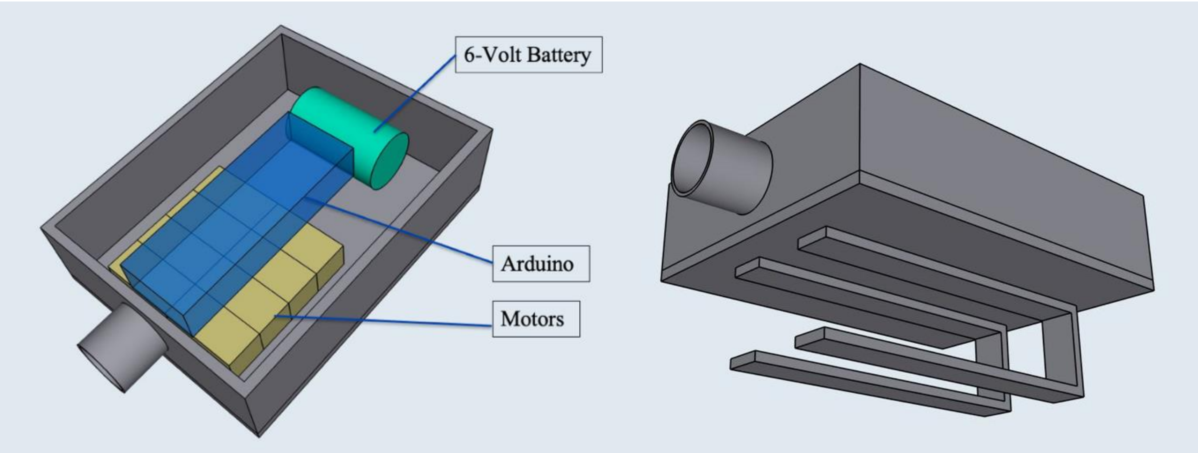

Figure 4: CAD of the external unit of the COMTRAD. The left shows the top view with the internal components visible, and the right shows the bottom view with the storage hooks below the box, where the collapsed housing can be stored when not in use. The external unit contains the 8 rotary motors (yellow), the Arduino board, and the battery. The CAD is for illustrative purposes, where the individual components in the box are shown with their sizes to scale but their details omitted.

5.1.3 *Movement (Actuator)*

The actuators implemented in the COMTRAD are targeted at achieving Aim 2 (probe movement). The housing of the COMRTRAD has 4 + 1 DOFs with 8 string actuators, 4 attached to the top plate of the probe holder and 4 to the bottom plate of the probe holder. The collapsing of the housing takes on 1 DOF along the vertical axis perpendicular to the skin plane (taken to be the z axis). The other 4 DOFs lie in the probe holder movement, in the form of the translational motion in the x and y axes parallel to the skin plane and the precession motion (rotation about the roll and pitch axes, where the yaw axis is parallel to the abovementioned z axis) to find the optimal CBFV signal. The 4 DOFs are needed to scan for the periodic CBFV signal using the translation and optimise the signal using the rotations. Figure 5 shows the 2 DOFs for the probe holder translation, and the rotation of the probe holder in one plane, which will be achievable in two planes as described above (2 DOFs). The force/tension applied/maintained at each string for the intended probe holder movement is also shown. A force is applied by the rotation of the motor shaft, while the tension is maintained by rubber dampers in the string holes of the hard plates of the surrounding shell. To view the force/tension needed for each of the 8 strings for each planned movement, refer to the supplementary video.

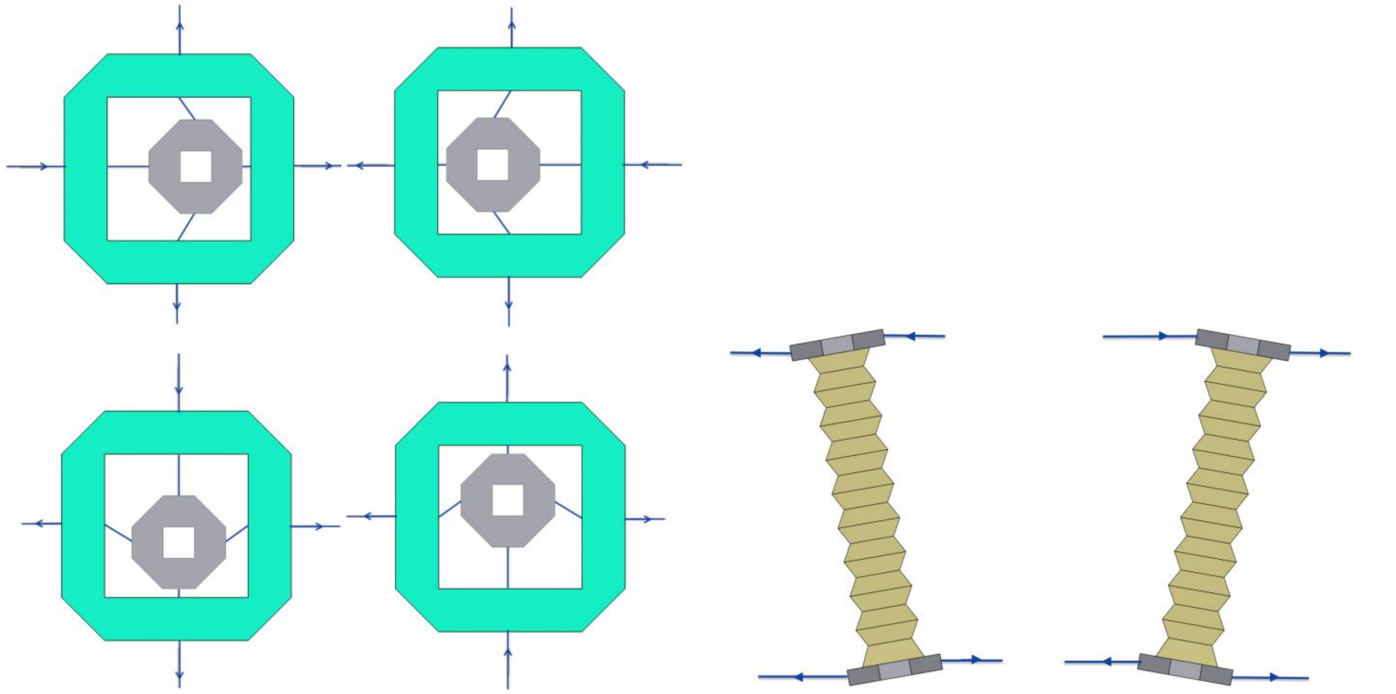

Figure 5: The 4 DOFs of the probe holder illustrated. The left schematic shows the top view of the 2 DOFs in translation motion of the probe holder. The right schematic shows the side view of 1 of the 2 DOFs in the rotational motions, The arrows on the strings represent the appropriate force/tension applied to the respective direction to execute the appropriate movement: opposite strings with opposing directional arrows indicate tension maintained, opposite strings with same directional arrows indicate force applied in the direction.

On the external unit end, the 8 strings are wound around its own pulley (1 cm diameter), which are mounted to the shaft of the 8 respective rotary motors (motor model: RS no: 752-2005). Between the housing and the external unit, each string will run inside a sheath and the sheaths are collectively channelled through a single cable for ease of management. Initially, we proposed 4 closed-loop strings instead of 8 individual strings, where each loop is controlled by a rotary motor. This produced a fully-actuated system (4 actuators for 4 DOFs) instead of the eventual over-actuated system (8 actuators for 4 DOFs).

The justification for this over-actuated system is that a closed string loop controlled by a single rotary motor is unable to release extra lengths of string (while maintaining tension) to facilitate probe holder movement, i.e. the probe holder will only be able to translate diagonally. The case where the longest length of string needed to be released within the surrounding shell is a unidirectional translation, where the strings orthogonal to the translation direction need to be extended up to 0.84 cm, as illustrated in Figure 6. If a string loop controlled with one rotary motor is used, it is incapable of releasing the strings in both directions. Therefore, we proposed the over-actuated system where the 8 strings are each controlled with a rotary motor as the simplest solution to the problem.

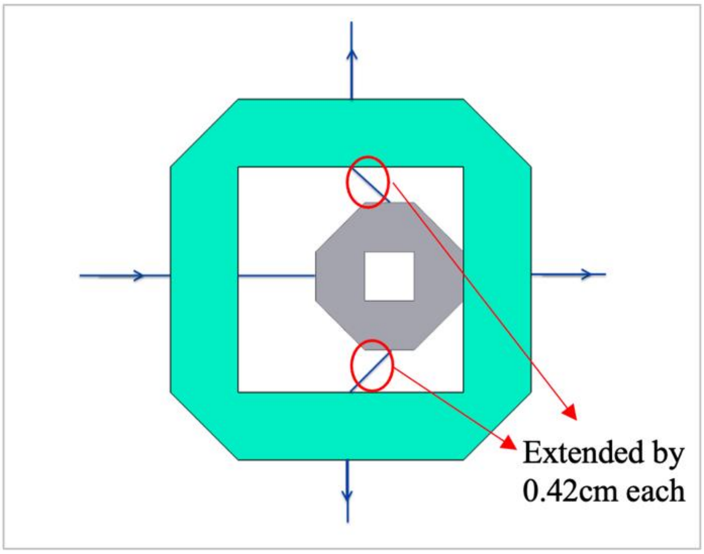

Figure 6: Top view of the unidirectional translation of the probe holder, which is the case where the longest length of string extension is needed in one axis. Relative to the central position the probe holder can take in the surrounding shell cavity, the strings above and below the probe holder in the diagram will have to extend by 0.42 cm each (determined via the Pythagoras theorem, rounded up to 2 d.p.), giving a total extension of 0.84 cm.

The rotary model used is the RS No.: 752-2005 (Figure 7) [13]. It has a RPM (low revolutions per minute) of 60, which allows us to achieve the intended translations and rotations of the probe holder. It is also light, weighing 10 g, and small, thus ideal for our application.

Figure 7: RS PRO brushed DC motor, 60 rpm, stock no. 752-2005 [13].

5.1.4 Sensing (Awareness)

The sensing portion of the COMTRAD is targeted at achieving Aim 3 (Positional Input). An IMU (model number ICM-20789), as seen in Figure 8 [14], would be mounted to the probe holder to determine its spatial position in relation to the surrounding shell. The spatial data is delivered to the controller via electrical wires that also run through the cable. The spatial data will be used in the scanning of the optimal CBFV signal and the stabilisation of the probe holder, which will be detailed in Section 5.1.5.

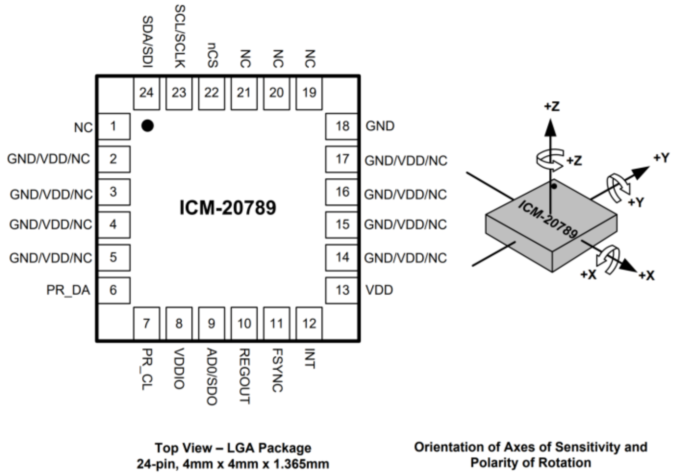

Figure 8: IMU model number ICM-20789 [14]. Shown here are the I/Os and the orientation of axes.

Also, the controller will require CBFV data live from the existing TCD machines as the data indicates if the stabilisation of the probe holder should be maintained or if the signal is lost and the planned movement of the probe holder will need to be executed. Currently, the data is manually read off the interface of the TCD machine as the exported dataset is an unreadable proprietary file format. For the complete implementation of the proposed device, the exported file will need to be investigated to extract the CBFV data. Subsequently, the exported file can be sent to the Arduino in the external unit wirelessly (via Bluetooth or Wi-Fi) or via a wired cable, and the data processing protocol can be written into the Arduino.

5.1.5 Controller (AI)

The controller implemented in the COMTRAD is targeted at achieving Aim 4 (Control System). A microcontroller (in this case the Arduino MKR GSM 1400, seen in Figure 9) can be used to store two main protocols written for the purposes of our proposed device: the stabilisation protocol and the scanning protocol. The controller takes in the CBFV data from the TCD machine and the spatial data from the IMU. From the CBFV data, if there is a presence of a periodic signal whose magnitude lies above a pre-set threshold (indicative of an optimal signal), the stabilisation protocol is executed; if there is an absence of said signal, the scanning protocol is executed.

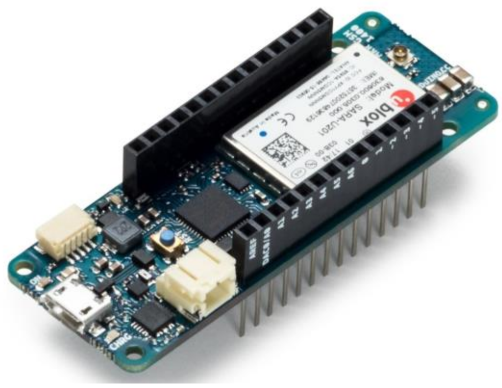

Figure 9: The Arduino MKR GSM 1400 [15].

Figure 10 shows the computational flow chart from the power on of the device. The stabilisation protocol involves a PID controller that takes in the spatial data of the probe holder. Before every stabilisation protocol, the scanning protocol would have been executed beforehand (either during the initial setting up of the COMTRAD or when the signal is lost) and the spatial data at the end of the scanning protocol would be used as the stability locus to maintain. In the presence of vibrations, the change in spatial data received would trigger the PID controller to enact the countering movement to maintain the stability locus. In the case where the housing is not mounted upright, i.e. the direction of the gravity needs to be taken into account, the protocol would use the accelerometer information from the IMU to counter the weight of the probe holder and probe accordingly with the appropriate increase in force/tension on the correct rotary motors. The PID parameters will have to be calibrated during the characterization of the COMTRAD. However, in the event the stabilisation of the probe holder fails due to unforeseen external factors, the scanning protocol will be executed to find the periodic signal again.

The scanning protocol is executed during the initial setting up of the COMTRAD on the patient's temporal window and when the periodic signal described above is lost. The planned movement of the probe holder will occur in two phases: translational, followed by rotational. During the translational phase, the probe holder is moved laterally across the skin plane in a zig zag manner (from scan boundary to boundary) till the periodic signal is found, and the probe holder stops translating in the skin plane. Subsequently, during the rotational phase, the probe holder is rotated about the roll and pitch axes simultaneously to produce a precession motion about the vertical axis at the planar position the probe holder stopped translating at. This purpose of this phase is to optimise the signal magnitude that was found previously in the translational phase. Once the optimum periodic signal is found, the spatial position of the probe holder is noted as the stability locus and the stabilisation protocol is executed.

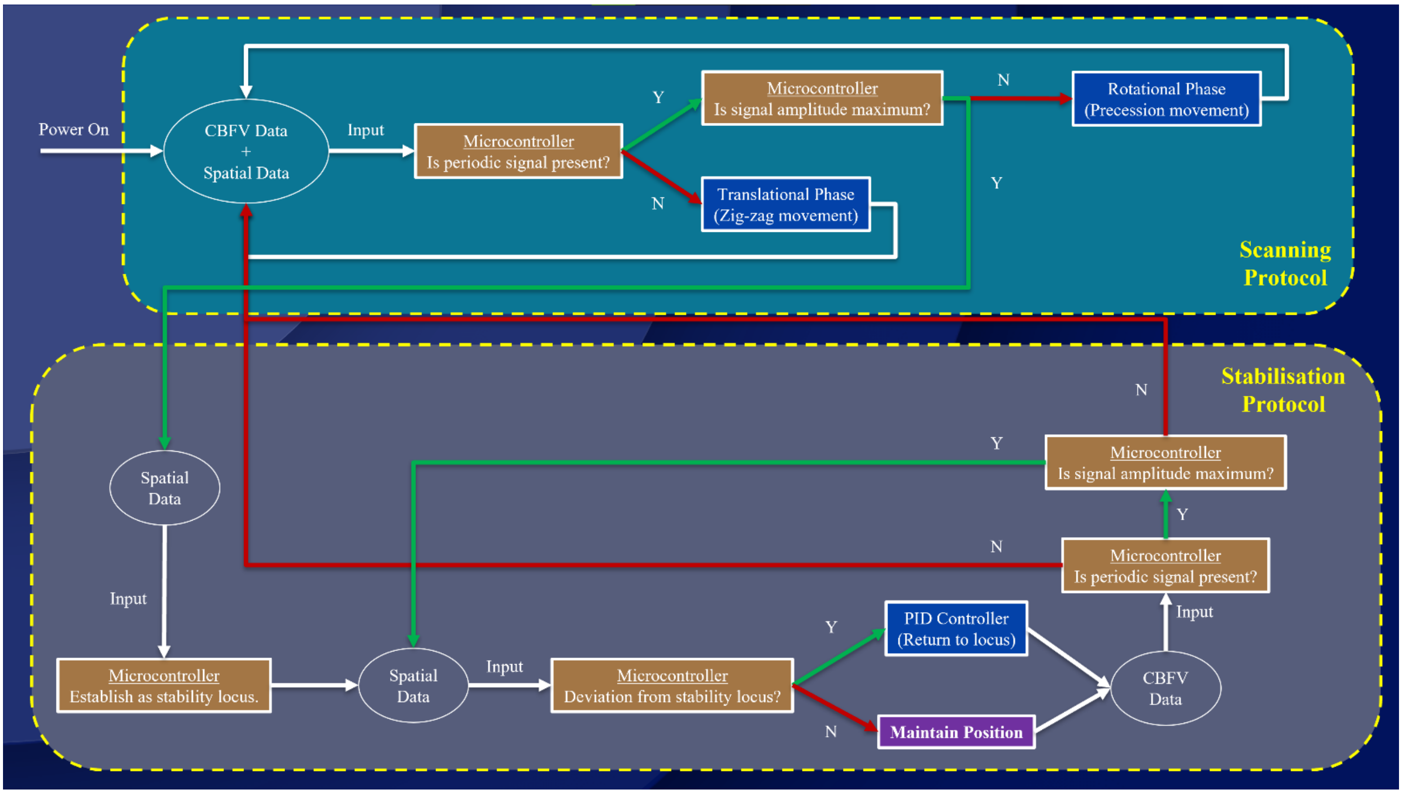

Figure 10: Computational flow chart of the scanning and stabilization protocols. White ovals represent a readout of data, brown boxes represent test conditions/value assignments done within the microcontroller, blue boxes represent execution of probe movement functions, purple box represents no action, red arrows represent a false condition, green arrows represent a true condition, and the yellow dashed rounded-rectangles enclose the scanning and stabilization protocols.

5.2 Specifications

Table 1: Relevant specifications in the COMTRAD design.

Components	Remarks	Dimensions
Strings	Inside surrounding shell	10 cm × 4
	Movement control	200 cm × 4
Springs	Uncompressed length	15 cm
	Compression limit	2 cm
Surrounding Shell	Compressed	8 × 8 × 2 cm with 5 × 5 × 2 cm cavity
	Expanded	8 × 8 × 10 cm with 5 × 5 × 10 cm cavity
Probe Holder	Compressed	3 × 3 × 2 cm with 1 × 1 × 2 cm cavity
	Expanded	3 × 3 × 10 cm with 1 × 1 × 10 cm cavity

Components	Remarks	Dimensions
Pulley	Diameter	1 cm
Motors	Model number	RS no: 752-2005
	Size	2 × 1.2 × 1 cm
	Rpm	60
Cable	Between external unit and wearable unit	90 cm
IMU	Model number	ICM-20789
	Size	0.4 × 0.4 × 0.137 cm
Arduino	Model number	MKR GSM 1400
	Size	1.25 × 7 × 2.5 cm
External Unit	Main body without storage	10 × 8 × 3 cm
	Main body with storage	10 × 8 × 5.5 cm

5.3 Materials

Table 2: Materials of relevant components in the COMTRAD design.

Component	Material/Model
Bellow Fold Sidewalls	Waxed Construction Paper
Hard Plates (Probe Holder & Surrounding Shell)	3D-Printed High-Density Polyethylene (HDPE)
Strings	Nylon
Pulley	3D Printed HDPE
Springs	Stainless Steel
String Hole Dampers	Rubber
String Sheath	Polyurethane
Cable Sheath	Polyurethane
IMU	ICM-20789
Arduino	MKR GSM 1400
Motors	RS No: 752-2005
Battery	CR-P2
External Unit Box	3D-Printed HDPE

5.4 Novelty

While there exist current devices that achieves the end goal in other ways, the COMTRAD's main novelty lies in its simplicity, storage capability, and adaptability to current TCD machines. The COMTRAD's functioning principle and materials needed are simple, which allows for easy manufacturing on a large scale for quick implementation to ambulatory settings. The storage capability of the entire device (set-up and external unit) meant that when not in use, the COMTRAD would not take up much space in the limited space available in an ambulance. The adaptability to current TCD machines would mean that hospitals can still utilise current TCD machines and not need to purchase separate TCD head devices in the market, which can be expensive to procure for the entire ambulance fleet.

5.5 Prototyping Approach

A low-fidelity prototype of the COMTRAD was made to test the movement mechanism of the probe holder. The origami template used for the folding of the side walls of the probe holder and surround shell can be found in the supplementary information. Figure 11 shows the expanded and collapsed versions of the set-up. The nylon strings attached to the probe holder were controlled manually, and the low-fidelity prototype was used to verify the 4 individual DOFs: translation in 2 axes and rotation in 2 axes. With the set-up fixed onto the ground surface, the appropriate application of force and maintenance of tension on the respective strings were used to execute the planned movements (refer to Figure 12 for the tension/force at each string). The viability of the movement in the translational phase and rotational phase for the scanning protocol was also tested. Also, the scanning area of the probe was determined. The results of the prototyping testing will be presented subsequently in Section 6.

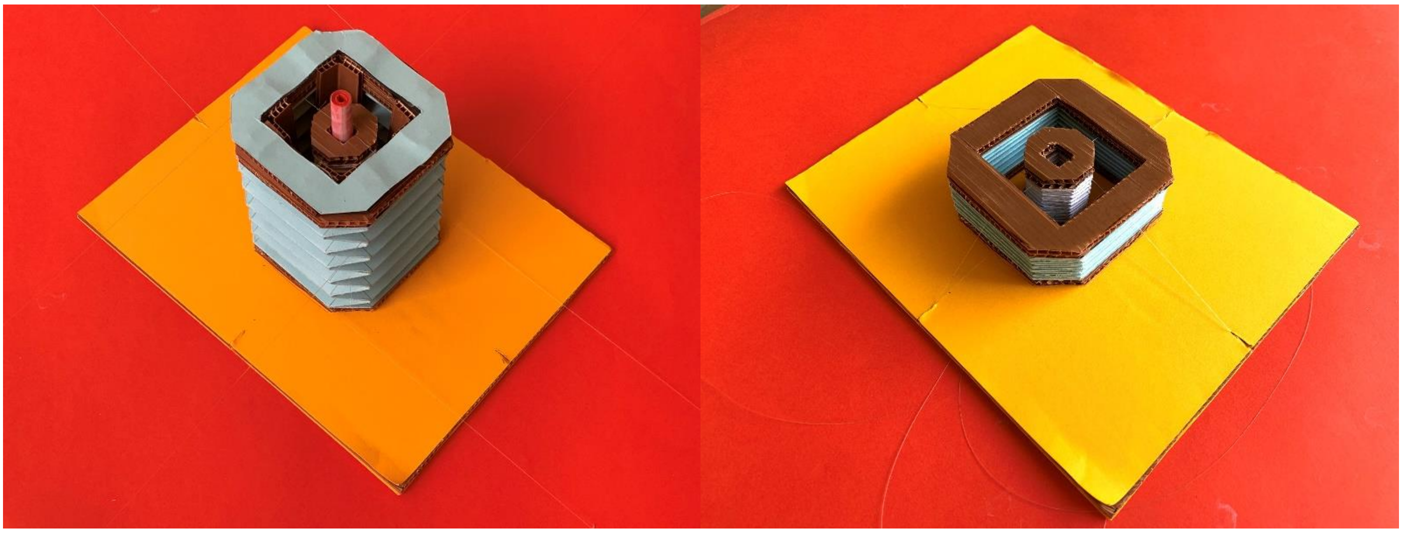

Figure 11: The low-fidelity prototype constructed to test the probe movement mechanism. On the left, the housing is in the extended form, and on the right, the housing is in the collapsed form.

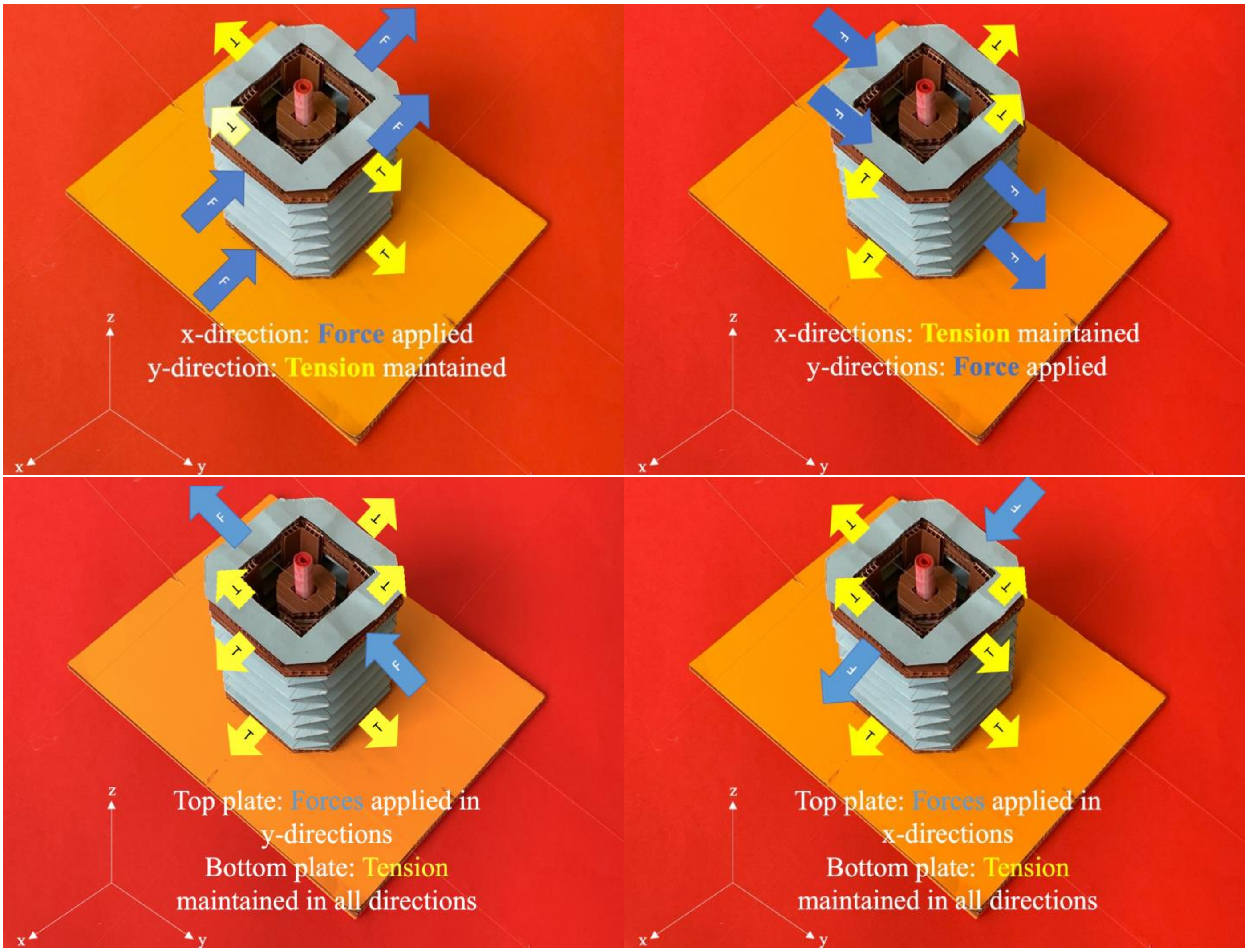

Figure 12: The forces and tension needed to be applied and maintain respectively for each of the eight strings. Short yellow arrows indicate tension (opposing force) maintain and longer blue arrows indicate force applied in the specified direction.

6 Results & Discussions

6.1 Probe Scanning Area

To determine the total scanning area that can be covered by the probe, the two extreme positions (Figure 13) the probe holder can reach are considered (the positions have rotational symmetry and hence only two of eight positions need to be considered). By rotating the two positions by 90° four times about the central axis of the surrounding shell and superimposing all the eight probe positions, the scanning area can be determined, as seen in Figure 14. The red (dashed) squares represent the probe positions shown in Figure 13B and the blue (dashed) squares represent the probe positions shown in Figure 13A; The yellow octagon (Figure 14) highlights the total scanning area, where the horizontal and vertical axes of the octagon are 3 cm and the individual (dashed) squares are 1 × 1 cm, giving a scanning area of 7 cm^2.

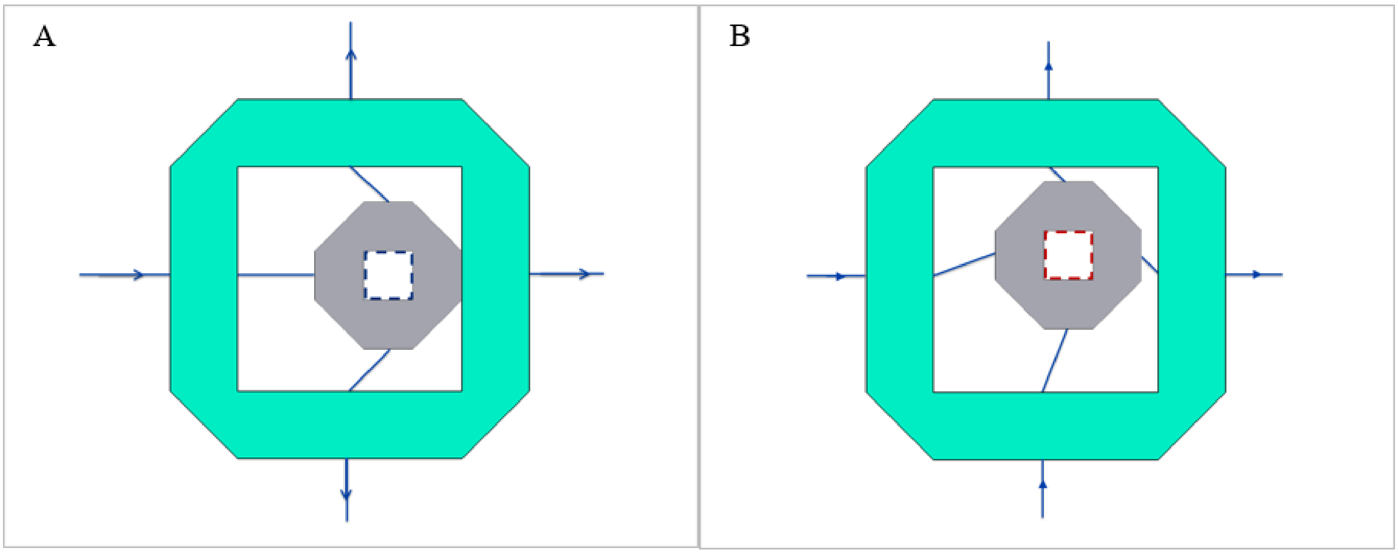

*Figure 13: Top view of the two unique extreme positions the probe holder can take; each unique extreme position has four spatial locations, but all four spatial locations are rotationally symmetrical with each other, hence the reduction to two unique extreme positions. The location of the probe in the side position (**A**) is represented by a blue dashed square, and the location of the probe in the corner position (**B**) is represented by a red dashed square. Likewise, the forces/tension applied/maintained on the respective arrows are represented with the arrows shown.*

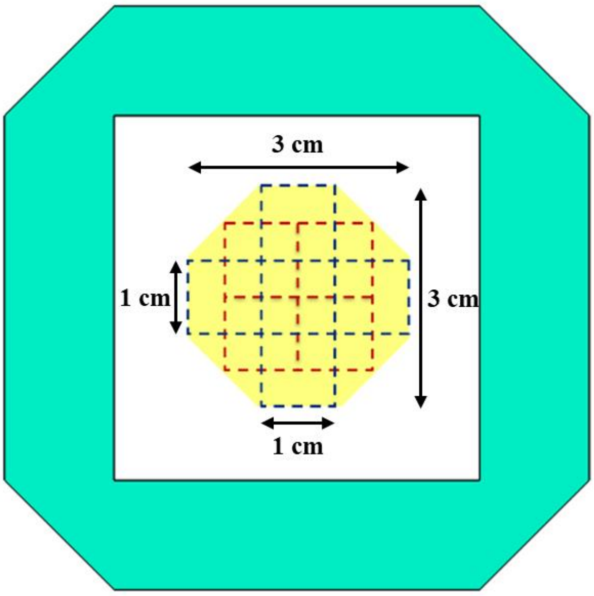

Figure 14: Scanning area covered by the probe. The blue/red squares represent the locations the probe can take in the extreme side/corner probe holder positions, as seen in Figure 13. The yellow octagon represents the total scanning area the probe can cover. Relevant dimensions of the scanning area are labelled. Note that the yellow octagon is not a regular octagon of 1 cm sides; In the diagram, it has 1 cm horizontal/vertical sides and $\sqrt{2}$ cm diagonal sides.

6.2 Probe Holder Movement

For the motors chosen, the movement speed of the COMTRAD can be determined. The motor (RS no: 752-2005) is a low RPM, high torque motor which provide the system sufficient force to move the probe holder precisely. With the diameter of the pulley D (1 cm) and RPM (60 rpm), the movement speed of probe holder can be calculated:

$$Movement\ Speed = \pi D \times \frac{RPM}{60} \approx 3.14\ cm/s^{-1}$$

The 4 DOFs of the probe holder, and the translational and rotational phase of the scanning protocol are verified using the low-fidelity prototype. The video demonstration of the verification process can be found in the supplementary video. The video documents the two single-axis translations in skin plane (2 DOFs), the two single-axis rotations (roll and pitch, 2 DOFs), and the translational and rotational phases of the scanning protocol. The testing (documented in the video) verifies the validity of the proposed probe holder movements.

6.3 Future Characterization & System Evaluation

Due to limitations in resources and time, a working high-fidelity prototype cannot be constructed. This section elaborates on the subsequent steps that need to be taken following the construction of the working high-fidelity prototype.

6.3.1 Characterization of Rotary Motors

It is essential for the rotary motors to pull and release the intended length of string in synchrony with the other motors. For instance, if the string motion on top and bottom hard plate are not synchronised, a purely translational motion would become a combination of translational and rotational motion. The chosen rotary motors have a rating of 60 rpm at 6V operating voltage. However, each motor has slight differences from one another due to manufacturing tolerances (e.g. the 60 rpm is subjected to an error of $\pm$12.5% [13]). As such, to obtain accurate control of all 8 motors, the characterization curve of each motor needs to be determined, i.e. the rpm-voltage curve for each motor. The controller can then accurately determine the respective voltage to each rotary motor for the intended probe holder movements.

6.3.2 Characterization of Probe Holder Movement

After characterizing each rotary motor, the controller can start to move the probe holder with a certain degree of accuracy. However, further calibration of the relationship between the controller and the 8 rotary motors is needed to move the probe holder as intended. When the probe holder can successfully move in test movements, the calibration of the relationship between the controller and the input spatial data from the IMU is needed. Afterwhich, the individual protocols should be tested.

For the scanning protocol, the testing should verify that the probe holder can successfully move as planned in the translational and rotational phases using the spatial data from the IMU. For the stabilisation protocol, a vibrating platform can be used to test the stabilisation of the probe holder. For this testing, the PID control parameters' values, i.e. the proportionality gain (K_P), integral gain (K_I), and derivative gain (K_D), should also be calibrated for the system. The K_P value would affect the response time of the counter-movements; the K_i value would affect the error within the stabilising process; the K_D value would affect the damping effect of the correction process (prevent over correction). While there exist models to determine the "ideal" PID parameter values, manual calibration is still necessary for the optimal values as each system is unique.

6.3.3 System Evaluation

Once the system can function as planned, the system will need to be evaluated for its performance. Adapting the system evaluation approach of Mackinnon et al. [5], patients suffering from ischemic stroke and healthy patients (control group) will be recruited for the evaluation. For each patient, the COMTRAD is mounted onto the patient and the CBFV data is monitored on the TCD machine by a trained operator. The system is evaluated based on its ability to search for the CBFV signal from the MCA, its ability to adjust the insonation angle to optimise the CBFV signal, and its ability to maintain the probe position when the patient is moving his head. The system performance can then be improved based on the evaluation results determined by a trained operator.

6.4 Potential Development

As part of the iterative design process, the COMTRAD design can be improved in various ways to better fulfil its individual aims.

6.4.1 Rigidization with Shape Memory Polymer

Currently, the housing of the COMTRAD is extended and rigidized through use of springs and strings at each corner of the surrounding shell (refer to Figure 3). However, the rigidization process can be replaced with the use of an electrically conductive shape memory polymer (SMP), that is also insulated on the surface, to construct the tetragonal bellow fold side walls, where the rigidization can be achieved thermally using Joule heating from a current. While there are also shape memory alloys (SMAs), SMPs have lower cost and density (hence lower weight), easy and fast shape training, and high bio-compatibility and degradability [16] [17]. Moreover, the rigidization of the housing can be controlled with a switch on the external unit.

6.4.2 Reduction in Motor Numbers with Redesigned Pulley

While the current design uses 8 rotary motors and 8 separate strings for the actuation of the probe holder, to reduce the over-actuated system to a fully-actuated system, the concept of 4 string loops controlled by 4 rotary motors can be revisited. As previously mentioned, such a design would not enable the necessary string extension while maintaining the tension; However, if the pulley is redesigned, the string extension would be possible.

Figure 15 illustrates the redesigned pulley fixed onto the shaft of the rotary motor, where the string loop ends on the opposite sides of the hard plate of the probe holder. In the instance where a force is applied in one direction, the rotary motor can rotate the string loop to exert the unidirectional force needed. In the instance where tension should be maintained and the string length needs to extend (e.g. by 0.42 cm on each side in Figure 6), the extension can be facilitated by the displacement of the outer ring of the pulley (Figure 15B). The force applied on the probe holder (on the sides orthogonal to the sides where the string extension is needed) will be larger than its counterpart in the current design, where the additional force is applied to displace the outer ring of the pulley and hence facilitate the string extension. Thus, although the complexity of the design and the difficulty in manufacturing the device has increased, the number of rotary motors would be halved, producing a fully-actuated system.

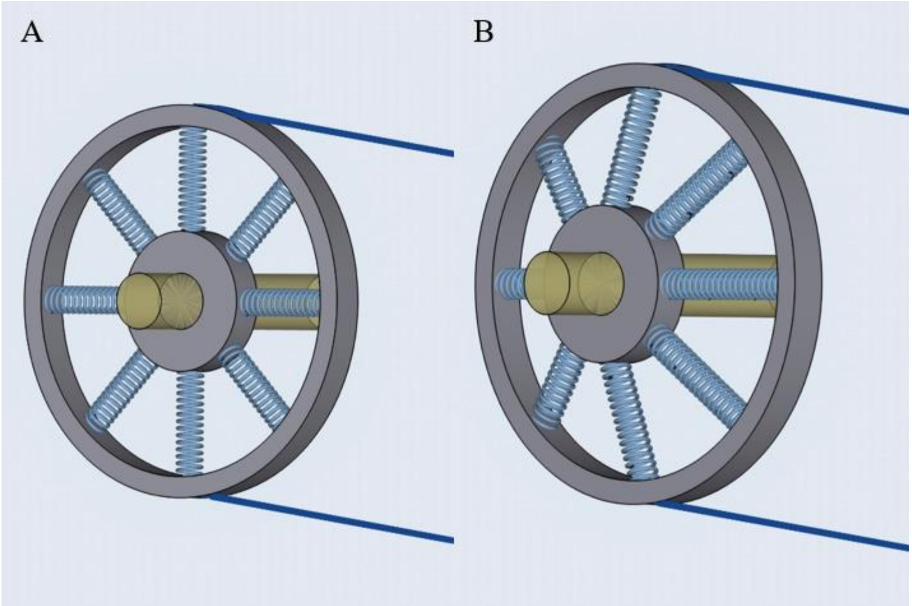

Figure 15: Concept illustration for the redesigned pulley, which consists of an inner and outer ring, and 8 springs between the two rings in the radial direction. The brown cylinder running through the inner ring of the pulley is the shaft of the rotary motor. A: All springs are of equal length and the motor shaft is in the center of the outer ring. No string extension in this instance. B: The springs are no longer of equal length, where the outer ring is skewed towards the direction of the string ends to facilitate the string extension. The displacement from the outer ring in A to the outer ring in B is equal to the length of string extended on one side of the probe holder, since the displacement will allow the strings to extend on both ends of the string loop.

6.4.3 Incorporating Neural Network to Identify Stroke

Currently, the COMTRAD is only designed to seek out the optimal CBFV signal of the MCA, and the non-trained operator will need to record the CBFV value for reporting to the medical staff at the hospital. However, since the COMTRAD already takes in the CBFV signal, if it is able to identify ischemic stroke in patients with an acceptable level of confidence (high sensitivity and specificity), then the information could be relayed to the medical staff ahead of time, in turn generating a faster response to the ischemic stroke in the patient to minimise tissue damage. Zhao et al. reported that the early administration of thrombolytic protein tissue plasminogen activator (tPA) to restore blood flow can prevent the infarct from expanding into the penumbra, allowing for the restoration of the injured but living cells of the penumbra to functionality [3].

For the COMTRAD to identify an ischemic stroke, a deep neural network can be used. The training, validation, and test sets can be obtained from the system evaluation, where the ground truth is determined from the medical condition of the patient (i.e. presence of ischemic stroke) and diagnosis of the trained operator. Overtime, as the data set becomes larger, and the sensitivity and specificity of the neural network in identifying ischemic strokes improve, the neural network can be stored on the Arduino, hence enabling the identification of ischemic strokes in ambulatory settings. This will further remove the burden of training from the operator and will closer approach the use case of an AED where the operator does not even need to know how to interpret the CBFV and will simply await the determination from the device.

7 Conclusion

The low-fidelity prototype of the COMTRAD has proven the validity of the probe holder movements and the viability of the design in its application. Naturally, more time and resources are needed to further the realisation of the proposed device, and the potential development to various areas of the system design were brought up. In future works, the discussed improvements to the COMTRAD can be implemented for better functionality and a design that is better suited for the established aims. Should the COMTRAD be able to deploy in ambulance settings, the ability to identify ischemic strokes in patients ahead of time can prove invaluable in minimising the tissue damage in the stroke patients, thereby improving the quality of life after treatment.

8 References

[1] National registry of Diseases Office , “Singapore Stroke Registry Annual Report 2018,” 9 June 2020.

[2] K. C. B. B. a. C. B. Janet E. Bray, “Paramedic Diagnosis of Stroke Examining Long-Term Use of the Melbourne Ambulance Stroke Screen (MASS) in the Field,” 2010.

[3] A. B. Chunyu Zhao, “Progranulin Protects Against the Tissue Damage of Acute Ischaemic Stroke,” *Brain,* vol. 138, no. 7, pp. 1770-1773, 2015.

[4] J. R. M. Camilo R. Gomez, “Transcranial Doppler Transducer Housing Stabilizer”. United States Patent 5070880, 10 December 1991.

[5] R. A. H. S. M. Andrew D. Mackinnon, “Long-Term Ambulatory Monitoring for Cerebral Emboli Using Transcranial Doppler Ultrasound,” *Stroke,* vol. 35, no. 1, p. 73–78, 2004.

[6] X. Y. ,. J. L. P. Z. a. X. W. Quanli Qiu, “A Robotic Holder of Transcranial Doppler Probe for CBFV Auto-Searching,” in *2013 IEEE International Conference on Information and Automation (ICIA),* Yinchuan, China, 2013.

[7] N. K. a. H. S. M. Jane Molloy, “Temporal Variability of Asymptomatic Embolization in Carotid Artery Stenosis and Optimal Recording Protocols,” *Stroke*, vol. 29, no. 6, p. 1129–1132, 1998.

[8] A. B. B. E. Z. M. E. R. Neil J. Sheehan, “Transcranial Doppler Probe Mounting Assumbly With External Compression Device”. United States Patent 5390675, 21 February 1995.

[9] P. C. Njemanze, “Intelligent Transcranial Doppler Probe”. United States Patent 6547737, 15 April 2003.

[10] R. J. W. Hiroyuki Suzuki, “Origami-inspired miniature manipulator for teleoperated microsurgery,” *Nature Machine Intelligence*, vol. 2, pp. 437-446, 2020.

[11] N. P. H. R. Hritwick Banerjee, “Single-Motor Controlled Tendon Driven Peristaltic Soft Origami Robot,” *Journal of Mechanisms and Robotics,* vol. 10, 2018.

[12] A. D. V. K. A. S. S. D. G. Mark Schenk, “Review of Inflatable Booms for Deployable Space Structures: Packing and Rigidization,” *Journal of Spacecraft and Rockets,* vol. 51, no. 3, pp. 762-778, 2014.

[13] RS PRO, “RS PRO Brushed DC Motor, 0.46 W, 6 V, 527 gcm, 60 rpm, 3mm Shaft Diameter,” n.d.. [Online]. Available: https://docs.rs-online.com/9598/A700000007082389.pdf. [Accessed 20 November 2020].

[14] TDK InvenSense, “7-Axis, High Performance Integrated 6-Axis Inertial and Barometric Pressure Sensor,” 30 January 2018. [Online]. Available: https://invensense.tdk.com/wp-content/uploads/2017/10/DS-000169-ICM-20789-TYP-v1.4.pdf. [Accessed 30 November 2020].

[15] Arduino, “Arduino MKR GSM 1400,” n.d.. [Online]. Available: https://store.arduino.cc/usa/mkr-gsm-1400. [Accessed 30 November 2020].

[16] H. Q. P. T. M. C. Liu, “Review of progress in shape-memory polymers,” *Journal of Materials Chemistry,* vol. 17, no. 16, p. 1543–1558, 2007.

[17] M. L. A. S. M. A. G. Jaronie Mohd Jani, “A review of shape memory alloy research, applications and opportunities,” *Materials and Design,* vol. 56, pp. 1078-1113, 2014.

[18] C. A. Giller and A. M. Giller, “A New Method for Fixation of Probes for Transcranial Doppler Ultrasound,” *Journal of Neuroimaging* , vol. 7, no. 2, 2016.

[19] Y. Chen, “A Reconfigurable Hybrid Actuator with Rigid and Soft Components,” in *2017 IEEE International Conference on Robotics and Automation (ICRA),* Singapore , 2017.

[20] R. W. A. B. M. M. a. H. S. M. Marisa Cullinane, “Asymptomatic Embolization in Subjects With Atrial Fibrillation Not Taking Anticoagulants,” *Stroke,* vol. 29, no. 9, p. 1810–1815, 1998.

[21] C. D. O. a. D. R. Andrew D. Marchese, “Autonomous Soft Robotic Fish Capable of Escape Maneuvers Using Fluidic Elastomer Actuators,” *Soft robotic,* vol. 1, 2014.

[22] Couzet, *Crouzet linear actuator data sheet.*

[23] R. V. Martinez, C. R. Fish, X. Chen and G. M. Whitesides, “Elastomeric Origami: Programmable Paper-Elastomer Composites as Pneumatic Actuators,” *Advanced Functional Materials,* vol. 22, 2012.

[24] T. H. J. R. Majid Taghavi, “Electro-ribbon actuators and electro-origami robots,” *Science robotics,* 2018.

[25] S. J. A. K. Ying Shi Teh, “Giant continuously-tunable actuation of a dielectric elastomer ring actuator,” *Extreme mechanics letters,* 2016.

[26] J. Park, “Numerical studies on origami dielectric elastomer actuator using Kresling pattern,” Embry-Riddle Aeronautical University, 2019.

[27] S. Esmaeeli, C. M. Hrdlicka, A. B. Bastos, J. Wang, S. Gomez-Paz and K. A. Hanafy, “Robotically assisted transcranial Doppler with artificial intelligence for assessment of cerebral vasospasm after subarachnoid hemorrhage,” *Journal of Neurocritical Care,* vol. 32, no. 40, 2020.

[28] A. Firouzeh, Y. Sun, H. Lee and J. Paik, “Sensor and actuator integrated low-profile robotic Origami,” *International Conference on Intelligent Robots and Systems (IROS),* 2013.

[29] J.⁚ r. W. Tobias Hemsel, “Survey of the present state of the art of piezoelectric linear motors,” *Ultrasonic 38,* pp. 37-40, 2000.

[30] S. P. D. R. C C Bishop and N. L. Browse, “Transcranial Doppler measurement of middle Cerebral artery Blood Flow Velocity: a validation study,” *Stroke,* vol. 17, no. 5, pp. 913-915, 1986.